Journal of Porous Media 10(1), 1–15 (2007)

The Stability of a Developing Thermal Front in a Porous Medium. I Linear Theory

Asma Selim and D. Andrew S. Rees

Department of Mechanical Engineering, University of Bath, Bath BA2 7AY, UK

ABSTRACT

In this paper, we analyze the stability of the developing thermal boundary layer that is induced by suddenly raising the temperature of the lower horizontal boundary of a uniformly cold semi-infinite porous domain. A full linear stability analysis is developed, and it is shown that disturbances are governed by a parabolic system of equations. Numerical solutions of this system are compared with the neutral stability curve obtained by approximating the system as an ordinary differential eigenvalue problem. Different criteria are used to mark the onset of convection of an evolving disturbance, namely, the maximum disturbance temperature, the surface rate of heat transfer, and the disturbance energy. It is found that these different measures yield different neutral curves. We also show that the disturbances have a favoured evolutionary path in the sense that disturbances introduced at different times or with different initial profiles eventually tend toward that common path.

Received April 15, 2005; Accepted December 20, 2005

NOMENCLATURE

E	energy of disturbance
g	gravity
i	$\sqrt{-1}$
k	wave number of disturbance
K	permeability
L	natural length scale
p	pressure
t	time
T	dimensional temperature
u	horizontal velocity
v	vertical velocity
x	horizontal coordinate
y	vertical coordinate

Greek characters

α	thermal diffusivity
β	expansion coefficient
δ	amplitude of disturbance
η	similarity variable
θ	nondimensional temperature
Θ	disturbance temperature
μ	dynamic viscosity
ρ	density
τ	scaled time
ψ	streamfunction
Ψ	disturbance streamfunction

Superscripts and subscripts

∞	ambient/initial conditions
$^-$	dimensional quantities
c	neutral/critical conditions
0	initial disturbance

INTRODUCTION

Convective flows in porous media are of interest in many varied situations, such as geothermal energy resource and oil reservoir modeling. The study of convection generated by heated horizontal surfaces embedded in a saturated porous medium has attracted extensive treatment in recent years. In the present paper, we are concerned with determining when an unsteady thermal boundary layer becomes unstable. Given a semi-infinite saturated porous domain that is uniformly cold, the lower surface has its temperature raised suddenly and the temperature field then evolves according to the standard complementary error function conduction solution, and there is no flow. However, in this situation, heavy fluid lies over relatively light fluid, and therefore, convective instabilities may arise. As the onset criterion in other contexts is given in terms of a Rayleigh number, which is itself defined in terms of a length scale, it is clear that a Rayleigh number that is based on the thickness of the developing hot region increases as time progresses. Therefore, one would expect to obtain a critical time for the onset of convection. The questions we wish to ask are (i) how do the wavelength, shape, and time of introduction of a thermal disturbance affect the time at which instability occurs, and (ii) can one define instability unambiguously?

A closely related topic is the Darcy-Bénard layer, which is composed of a horizontal layer of uniform thickness porous material that is saturated with a fluid and heated from below. Horton and Rogers (1945)

and Lapwood (1948) were the first to provide linear stability analyses in order to determine the onset criterion for buoyancy-driven motion in such layers. Both papers assumed Darcy's law subject to the Boussinesq approximation as the mathematical model, and this simplifies the stability analysis. It is well known that convection in such an idealized setting takes place whenever the Darcy-Rayleigh number is above $4\pi^2$ in a horizontally unbounded layer and the corresponding convection pattern at moderately supercritical Darcy-Rayleigh numbers takes the form of two-dimensional rolls with a square cross section. Of course, the situation is more complicated than this in reality, for disturbances may not contain this preferred pattern as a Fourier component. In addition, neither Darcy's law nor the Boussinesq approximation apply in all circumstances, and this can affect not only the onset criterion, but also the pattern of convection that is observed. For further details, see the review chapter by Rees (2000) and the lecture notes of Rees (2001a).

The present paper considers the stability of a thermal boundary layer that varies in time but is uniform, horizontally, rather than a steady one whose thickness varies with distance from a leading edge. In the porous medium context, many authors have considered the linearized stability properties of the latter type of thermal boundary layer. Generally, the basic convecting state is steady in time but nonuniform in space. Most attention has been given to either horizontal or generally inclined boundary layer flows. Although the basic states are self-similar (see the papers by Cheng and Chang, 1976, and Cheng and Minkowycz, 1977), they are not spatially uniform. Therefore, a full linearized stability analysis has to follow one of the following options: (i) the equations remain elliptic, (ii) an ad hoc approximation is made that reduces the elliptic equations to an ordinary differential eigenvalue form, or (iii) the near-vertical limit is taken, for which the elliptic equations may approximated consistently by a parabolic system. To date, only three papers have followed option (i) and these are Rees and Bassom (1993), who showed that two-dimensional instabilities become chaotic immediately for the horizontal boundary layer, and Rees (1993) and Lewis et al. (1995), who show that the vertical boundary layer is always stable. Option (ii) has been followed by a very large number of authors (see the reviews by Rees, 1998 and 2002a, for details) who have invoked a great variety of extensions to Darcy's law. As shown by Storesletten and Rees (1998), such approximations are inherently self-defeating for the boundary layer approximation (which assumes that x, the distance from the leading edge, is asymptotically large) is employed to obtain the basic flow, whereas the neutral distance is computed to be rather small, and certainly, within a region where the boundary layer approximation is poor. Finally, option (iii) is a special case that is peculiar to porous medium boundary layers, for the critical distance recedes from the origin as the inclination of the heated surface nears the vertical. Therefore, it has proved possible to get very detailed and accurate solutions of the resulting parabolic system of disturbance equations for both the linearized and fully nonlinear cases, for the boundary layer approximation applies consistently to the disturbance equations; see Rees (2001b,2002b,2003).

In the present paper, the basic state is computed exactly, unlike the boundary layer flows reviewed above. However, all the papers published on this topic have, to date, introduced approximations that are similar to option (ii). The main aim here is to determine the stability properties using a method closely allied to both options (i) and (iii), and to compare that to an option (ii) approximation. In other words, we solve the full linearized stability equations, which are elliptic in space and parabolic in time, and compare those results to an approximate ordinary differential system that corresponds to setting time derivatives arbitrarily to zero in order to mimic neutral stability.

The corresponding stability analysis for suddenly heated clear fluid systems has also been investigated to a large extent. The first theoretical analysis of a time-dependent thermal instability problem in a clear

fluid was by Morton (1957). In the case of rapid heating from below in a layer of finite thickness, the basic conduction solution is still time dependent when buoyancy-driven convection sets in. The classical Bénard convection problem then corresponds to when this basic temperature profile has become fully developed. This kind of thermal instability in fluid layers was also studied by Foster (1965) who treated this time dependency as an initial value problem. His method, called amplification theory, requires both the initial conditions and an amplification factor to mark the onset of convection. Another method, called propagation theory, has been used by Hwang and Choi (1996), Choi et al. (1998), and Kim et al. (1999) for convection in clear fluids, and by Kim et al. (2004) for the instability of the flow induced by an impulsively started rotating cylinder. This theory employs the thermal penetration depth as a length scaling factor and then the linearized stability equations are transformed into self-similar form. This results in an ordinary differential eigenvalue problem to solve for the critical time on invoking the principle of the exchange of stabilities. Bassom and Blennerhassett (2002) studied impulsively generated convection in a semi-infinite fluid layer above a heated flat plate considering both linear and nonlinear stability, where they used the quasi-steady approximations to generate linear stability theory neutral curves. They presented the linear theory results for the temperature profile, which is generated by a step change in the plate temperature, an asymptotic solution for strongly nonlinear roll-cell convection is used for the case of an impulsively applied heat flux at the plate.

Kaviany (1984) extended the amplification theory into the porous medium context with the inclusion of internal heat generation in a finite thickness layer. Kim et al. (2002) also considered this internal heat generation problem where the basic state was still time dependent and employed amplification theory. Later, Kim et al. (2003) considered what is essentially the same problem as is investigated here, although their application is to an oil-saturated medium with gas diffusion from below. Recently Kim and Kim (2005) have considered the onset of convection in a porous layer where the temperature of the lower surface increases linearly with time. Again, amplification theory is applied.

Unlike the above-mentioned papers, we do not rely on approximate theory to give a critical time for the onset of convection in a porous region that is suddenly heated from below. Rather, we solve the full linearized disturbance equations numerically in order to attempt to obtain a neutral curve relating the critical time and the disturbance wave number. The critical time is found to depend on a multitude of factors, including the time, shape, and wave number of the initiating disturbance and the manner in which one attempts define instability. The resulting curves are then compared with the results of approximate theory, and conclusions are drawn. In general, we find that convection occurs much earlier than is predicted by the approximate theories.

GOVERNING EQUATIONS AND BASIC SOLUTION

We are considering the instability of an initially quiescent semi-infinite region of saturated porous medium at the uniform temperature T_∞, whose lower boundary has its temperature raised suddenly to a new uniform level T_w. The porous medium is considered to be homogeneous and isotropic. We assume that the flow is governed by Darcy's law modified by the presence of buoyancy and subject to the Boussinesq approximation. The fluid and the porous matrix are also assumed to be in local thermal equilibrium when considering the thermal energy equation. It is not necessary to consider the fully three-dimensional equations since the linearized disturbance equations may always be Fourier decomposed into two-dimensional components of the form we consider here. Thus, we begin our analysis with a two-dimensional system. Thus, the governing equations of motion and temperature field for buoyancy-driven convection are expressed as

$$\frac{\partial \bar{u}}{\partial \bar{x}} + \frac{\partial \bar{v}}{\partial \bar{y}} = 0 \tag{1a}$$

$$\bar{u} = -\frac{K}{\mu}\frac{\partial \bar{P}}{\partial \bar{x}} \tag{1b}$$

$$\bar{v} = -\frac{K}{\mu}\frac{\partial \bar{P}}{\partial \bar{y}} + \frac{\rho g \beta K}{\mu}(T - T_\infty) \tag{1c}$$

$$\frac{\partial T}{\partial \bar{t}} + \bar{u}\frac{\partial T}{\partial \bar{x}} + \bar{v}\frac{\partial T}{\partial \bar{y}} = \alpha\left(\frac{\partial^2 T}{\partial \bar{x}^2} + \frac{\partial^2 T}{\partial \bar{y}^2}\right) \tag{1d}$$

In these equations, $\bar{x}$ is the coordinate in the horizontal direction while $\bar{y}$ is vertically upward. The corresponding velocities are $\bar{u}$ and $\bar{v}$, respectively. All the other terms have their usual meaning for porous medium convection: K is the permeability, μ is the dynamic viscosity, and ρ is the density of the fluid at the ambient temperature $T = T_\infty$. The heated horizontal surface is held at the temperature T_w, where $T_w > T_\infty$. Finally, the quantities g, β, and α are gravity, the coefficient of cubical expansion, and the thermal diffusivity of the saturated medium, respectively.

When nondimensionalizing the variables in Eq. (1), it has been assumed that the porous medium Rayleigh number, $\mathrm{Ra} = \rho g \beta K L(T_w - T_\infty)/\mu\alpha$, has been set equal to 1. Such an assumption is discussed in some detail in the review by Rees (1998), and it is equivalent to defining a natural length scale based on the fluid and matrix properties; thus, a nondimensional length of precisely 1 is equivalent to the dimensional length L given by

$$L = \frac{\mu\alpha}{\rho g \beta K (T_w - T_\infty)} \tag{2}$$

A rough idea of what this length scale might represent in practice may be gained by employing the following data representing water saturating soil at a mean temperature of 25 K: $\mu = 8.91 \times 10^{-4}$ kg/ms, $\alpha = 1.44 \times 10^{-7}$ m^2/s, $\rho = 997$ kgm^3, $g = 9.81$ m/s^2, $\beta = 2.6 \times 10^{-4}$/K, $K = 10^{-12}$ m^2, $T_w - T_\infty = 10$ K; this yields a length scale of $L \simeq 5$ m.

Equations (1a)–(1d) may now be nondimensionalised using the following transformations:

$$\bar{t} = \frac{L^2}{\alpha}t, \quad (\bar{x}, \bar{y}) = L(x, y), \quad (\bar{u}, \bar{v}) = \frac{\alpha}{L}(u, v)$$
$$\bar{P} = \frac{\alpha\mu}{K}p, \quad T = T_\infty + \Delta T\, \theta \tag{3}$$

to yield

$$\frac{\partial u}{\partial x} + \frac{\partial v}{\partial y} = 0 \tag{4a}$$

$$u = -\frac{\partial p}{\partial x} \tag{4b}$$

$$v = -\frac{\partial p}{\partial y} + \theta \tag{4c}$$

$$\frac{\partial \theta}{\partial t} + u\frac{\partial \theta}{\partial x} + v\frac{\partial \theta}{\partial y} = \frac{\partial^2 \theta}{\partial x^2} + \frac{\partial^2 \theta}{\partial y^2} \tag{4d}$$

The appropriate boundary conditions are

$$y = 0: \ v = 0, \ \theta = 1 \text{ and } y \to \infty: \ v, \theta \to 0 \tag{4e}$$

while $\theta = 0$ everywhere for $t < 0$.

After eliminating the pressure p between Eqs. (4b) and (4c) and on introducing the streamfunction ψ defined according to

$$u = -\frac{\partial \psi}{\partial y} \qquad \text{and} \qquad v = \frac{\partial \psi}{\partial x} \tag{5}$$

then the continuity equation is satisfied, and Eqs. (4b)–(4d) reduce to the pair

$$\frac{\partial^2 \psi}{\partial x^2} + \frac{\partial^2 \psi}{\partial y^2} = \frac{\partial \theta}{\partial x} \tag{6a}$$

$$\frac{\partial \theta}{\partial t} + \frac{\partial \psi}{\partial x}\frac{\partial \theta}{\partial y} - \frac{\partial \psi}{\partial y}\frac{\partial \theta}{\partial x} = \frac{\partial^2 \theta}{\partial x^2} + \frac{\partial^2 \theta}{\partial y^2} \tag{6b}$$

which are to be solved subject to the boundary conditions,

$$y = 0: \ \psi = 0, \ \theta = 1 \text{ and } \ y \to \infty: \ \psi, \theta \to 0 \tag{6c}$$

and the initial condition that

$$\psi = \theta = 0 \quad \text{at} \quad t = 0 \tag{6d}$$

Therefore, at $t = 0$, the temperature of the lower boundary of the semi-infinite region of porous medium is raised suddenly from 0 to 1, where it remains for all $t > 0$.

For the basic profile, we note that the equations may admit solutions that are uniform horizontally. Given the form of Eq. (6a), an x-independent temperature field yields a no-flow state. Therefore, the

thermal energy equation of the purely conducting state is

$$\frac{\partial \theta}{\partial t} = \frac{\partial^2 \theta}{\partial y^2} \tag{7}$$

and the analytical solution is

$$\theta = \text{erfc}\,(\eta) = \frac{2}{\sqrt{\pi}} \int_{\eta}^{\infty} e^{-\xi^2}\, d\xi, \tag{8}$$

where

$$\eta = \frac{y}{2\sqrt{t}} \tag{9}$$

In this paper, we choose to consider disturbances to the basic profile given in (8) by first transforming the governing equations into the coordinate system (η, τ), where η is given above, and $\tau = \sqrt{t}$. Eqs. (6a) and (6b) become

$$4\tau \frac{\partial^2 \psi}{\partial x^2} + \frac{1}{\tau} \frac{\partial^2 \psi}{\partial \eta^2} = 4\tau \frac{\partial \theta}{\partial x} \tag{10a}$$

$$2\tau \frac{\partial \theta}{\partial \tau} + 2\tau \Big(\frac{\partial \psi}{\partial x} \frac{\partial \theta}{\partial \eta} - \frac{\partial \psi}{\partial \eta} \frac{\partial \theta}{\partial x} \Big) = 4\tau^2 \frac{\partial^2 \theta}{\partial x^2} + \frac{\partial^2 \theta}{\partial \eta^2} + 2\eta \frac{\partial \theta}{\partial \eta} \tag{10b}$$

We note that the coefficient of $\partial\theta/\partial x$ on the right-hand side of (10a) plays the role of a Rayleigh number. The reason is that a Rayleigh number based on the thickness of the developing thermal boundary layer is exactly proportional to $\tau = \sqrt{t}$. Therefore, it is clear that the strength of the buoyancy forces increases as time progresses since the thickness of the region over which the temperature varies from 1 on the lower boundary to a nominal value, such as 0.01, also increases with time.

PERTURBATION ANALYSIS

We now perturb the basic solution given by (8) and by $\psi = 0$ in order to assess the stability properties of the developing thermal layer. The perturbation is assumed to be small in magnitude, and therefore, we set

$$\psi(\eta, x, \tau) = \delta \Big[i\Psi(\eta, \tau) e^{ikx} + \text{c.c.} \Big] \tag{11a}$$

$$\theta(\eta, x, \tau) = \text{erfc}\,\eta + \delta \Big[\Theta(\eta, \tau) e^{ikx} + \text{c.c.} \Big] \tag{11b}$$

where c.c. denotes complex conjugate. Here, the value k is the horizontal wave number of the roll-like disturbances and their amplitude δ is assumed to be sufficiently small that higher powers may be neglected. The resulting linear equations for Ψ and Θ are

$$\Psi'' - 4\tau^2 k^2 \Psi = 4\tau^2 k \Theta \tag{12a}$$

$$2\tau \Theta_\tau = \Theta'' + 2\eta \Theta' - 4\tau^2 k^2 \Theta - \frac{4}{\sqrt{\pi}} \tau k e^{-\eta^2} \Psi \tag{12b}$$

where primes denote derivatives with respect to η. The boundary conditions to be satisfied by these disturbances are that

$$\eta = 0: \ \Psi = \Theta = 0 \ \text{ and } \eta \to \infty: \ \Psi, \Theta \to 0 \tag{12c}$$

This system of equations is parabolic in τ; and thus an exact linearized analysis must consist of determining how disturbances evolve with time after a disturbance has been initiated. Therefore, Eqs. (12) represent both an option (i) method and an option (iii) method, as defined in the Introduction, by being both parabolic and exact.

It is possible to vary not only the wave number k of the disturbance, but also its profile and its initiation time, denoted by τ_0. On the other hand, approximate theories usually involve neglecting the time derivative, which results in an ordinary differential eigenvalue problem for the critical time, as represented by τ here. Although comparisons between the parabolic system and the quasi-steady-state approximate system are made later, it is important to note that the solutions to the approximate steady-state system depend on whether the y or η coordinate is used. The reason for the difference is that the $2\eta\Theta'$ term in (12b) arises from the Θ_t term when changing coordinates from y to η. Therefore, the steady-state assumption is different in the two coordinate systems.

NEUTRAL CURVES

As already mentioned, Eqs. (12a) and (12b) have a single τ-derivative, which implies that the linear

development of disturbances to the basic flow is governed by a parabolic system. Indeed, while Θ varies according to (12b), the streamfunction Ψ reacts instantly to changes to Θ. Therefore, the appropriate way of analyzing instability must be to introduce a disturbance into the boundary layer at some point in time and to monitor its evolution with τ. However, as a guide to what to expect from such a simulation, we will obtain a reference neutral curve by neglecting the τ-derivative in (12b). Therefore, Eqs. (12a) and (12b) reduce to an ordinary differential eigenvalue problem for the scaled critical time τ. This approximate system is given by

$$\Psi'' - 4\tau^2 k^2 \Psi = 4\tau^2 k \Theta \tag{13a}$$

$$\Theta'' + 2\eta\Theta' - 4\tau^2 k^2 \Theta - \frac{4}{\sqrt{\pi}}\tau k e^{-\eta^2}\Psi = 0 \tag{13b}$$

which is to be solved subject to the boundary conditions given in (12c). However, since these boundary conditions are homogeneous, it is essential to force a nonzero solution by setting $\Theta'(0) = 1$, for example. This extra boundary condition requires an extra equation given by

$$\tau' = 0 \tag{14}$$

A suitably modified version of the Keller-box method has been used to solve this eigensystem (see Lewis et al. 1997, for details). Briefly, Eqs. (13) are discretized using central differences in order to form a nonlinear set of algebraic equations for the eigenvalue τ, in terms of the chosen value of the wave number k. In our computations, we used a uniform grid of 201 points in the range $0 \leq \eta < 10$. The results of our computations yield the neutral curves, which are shown in Figs. 1a and 1b.

Figure 1a shows the variation of τ with τk and also shows the standard single-minimum curve typical of most thermoconvective instabilities. The horizontal coordinate, τk, may be regarded as being a wave number relative to the developing thickness of the basic thermal boundary layer that is proportional to τ. In a different computation, we have determined that the critical time and its associated wave number, which is the minimum point on the curve displayed in Fig. 1a, are given by

$$\tau_c = 12.944356, \qquad k_c = 0.069623 \tag{15}$$

These values were obtained to the given accuracy by solving (13) augmented by the system obtained by differentiating (13) with respect to k and by setting

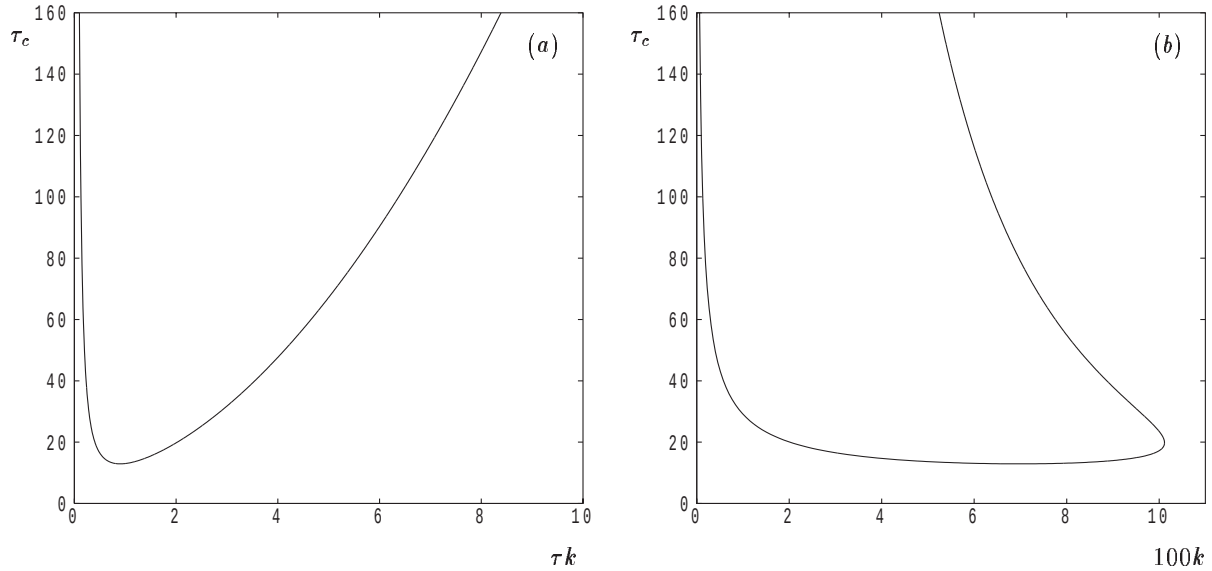

Figure 1. Neutral stability curve: **a)** τ_c against τk; **b)** τ_c against k

$\frac{\partial \tau}{\partial k} = 0$; in this case, we used a fourth-order Runge-Kutta code together with a standard shooting method for this two-point boundary value problem.

Given that k is fixed for any chosen disturbance, the variation of τ with k is shown in Fig. 1b. In this figure, those points that are below and to the right of the neutral curve correspond to stability, whereas instability corresponds to points inside the curve. In practice, of course, time increases and, therefore, this curve shows that we expect all disturbances to decay when $\tau < 12.944356$; however, at later times some disturbances will grow, but only if $k < 0.101053$, which corresponds to the turning point on the right-hand side of the curve. This maximum value of k was found using the same Runge-Kutta/shooting method code, but with Eqs. (13) supplemented by a system obtained by differentiating (13) with respect to τ and by setting $\frac{\partial k}{\partial \tau} = 0$. It is also clear that this approximate method predicts that all disturbances decay when $k > 0.101053$.

For this type of approximation, neutrality corresponds to when the whole θ profile achieves a minimum value as either τ or t increases. This is, of course, an artificial constraint, and has the effect of 'stiffening' the system of equations, thereby giving conservative estimates of the critical time. On the other hand, a solution of the full parabolic system allows the temperature profile to evolve freely subject to no constraints other than the boundary conditions. Therefore, it is an *a priori* expectation that the parabolic simulation will yield instability at earlier times, and will yield a larger region of instability.

PARABOLIC SIMULATIONS

The rest of the present paper is devoted to the presentation of solutions of the full linearized disturbance Equations (12) and discussion of their significance. Stability characteristics inferred from these solutions will also be compared with the quasi-steady stability analysis shown in Fig. 1.

Parabolic simulations of the system given by Eqs. (12) were undertaken using the Keller-box method, first introduced by Keller and Cebeci (1971). However, we use a backward difference discretization in τ, rather than a central difference approximation, in order to maximize numerical stability. In the computation, uniform grids in both the τ and η directions were used with 991 intervals specified in the range $0 \leq \tau \leq 100$ and 201 intervals in the range $0 \leq \eta \leq 10$. The general procedure we followed was to introduce an initial disturbance profile for the temperature field at a chosen initiation time τ_0 and with a specified wave number k. We note that the corresponding initial Ψ profile is given uniquely by the solution of Eq. (12a).

As our aim here is to study the stability characteristics of the thermal boundary layer after introducing thermal disturbances, we are interested in the manner in which the cells evolve in time as a function of the initiation time of the disturbance, its initial spanwise profile, and its wave number. Our datum case is the temperature profile, $\Theta = \eta e^{-3\eta}$, which is introduced at $\tau_0 = 1$, a time that is well before instability is expected to occur. In turn, we shall alter the profiles, the wave numbers, and initiation times in order to gain a comprehensive picture of the stability characteristics of the developing thermal field.

The status of the evolving disturbances (i.e., whether they are decaying or growing) was monitored by the computation of the following quantities: (i) the maximum temperature, (ii) the surface rate of heat transfer, and (iii) the thermal energy of the disturbance. For (i) the maximum temperature at each scaled time τ was obtained by locating the maximum value over all grid points, fitting a parabolic curve to that point and its two nearest neighbours and finding the maximum value on that curve. For (ii), the surface rate of heat transfer is measured in terms of both Θ_y and Θ_η at $\eta = 0$. Finally, for (iii), the thermal energy of the disturbance is defined according to

$$E = \tfrac{1}{2} \int_0^\infty \Theta \, dy = \tau \int_0^\infty \Theta \, d\eta \tag{16}$$

We note that all three of these measures yield identical results for spatially uniform, steady basic states,

such as for the classical Bénard problem and its analogous porous medium problem, the Darcy-Bénard layer. But we will show that these measures give different results for the present unsteady basic state.

Figure 2 shows the evolution with τ of the disturbance shapes, $\Theta \cos kx$ and $\Psi \sin kx$, for the datum initial profile with $k = 0.06$ and $\tau_0 = 10$. Each frame displays contours corresponding to 20 equally spaced subintervals between their respective maximum and minimum values. The isotherms and streamlines are displayed in both (x, y)-space and (x, η)-space.

Figures (2a) and (2b) show the isotherms and streamlines, respectively, in (x, y)-space. The heights of the individual frames correspond to the full computational and physical domain, $0 \leq \eta \leq 5$ in this case (although the remainder of the paper uses $0 \leq \eta \leq 10$), and the aspect ratios shown have unit distances in each direction correspond to the same distances within the figure. In the $\tau = 20$ case, for example, the horizontal scale is $x_{\max} = 2\pi/k \simeq 104.7$ while $y_{\max} = 2\eta_{\max}\tau = 100$, and the flow domain has almost exactly a unit aspect ratio.

Figures (2a) and (2b) clearly show that the thickness of both the temperature and velocity disturbances increase in size as time progresses. This, perhaps, is not surprising becous the thickness of the thermal boundary layer increases with time and because the fluid is not bounded above. However, when viewed in (x, η)-space, it is clear that the disturbance tends to compress slightly toward the heated surface as τ increases. The compression may be understood in relation to the fact that Eq. (12b) includes the term $-4\tau^2 k^2 \Theta$. When τk is large, the magnitude of this term must balance with the highest derivative term, Θ''. This means that the thickness of the developing disturbance must be of $O(\tau^{-1})$ in terms of the η coordinate. In terms of y, this means that the disturbance tends toward a uniform thickness at very large times.

Figures 3a and 3b represent the evolution of the disturbance energies E for different values of k satisfying $k \leq 0.07$ and $k > 0.07$, respectively. The initiation time is again $\tau_0 = 1$. The critical values of τ, which are the maxima and minima on each curve, are also emphasized using filled circles in order to indicate clearly how τ_c varies with k. For all wave numbers, the disturbance energy decays at first in a manner that is independent of the wave number. The reason for this is that (12b) may be approximated by

$$2\tau\Theta_\tau = \Theta'' + 2\eta\Theta' \tag{17}$$

when τk is small, and therefore, the initial evolution is not a function of k. At later times, when τk is no longer small, the disturbance energy becomes highly dependent on the value of k.

Focusing now on the critical times, Fig. 3a shows that the critical value of τ, τ_c, is a decreasing function of k when k is less than or equal to roughly 0.07. At higher wave numbers, τ_c increases as k increases, which is seen in Fig. 3b. Very similar curves may be drawn for the other measures of the strength of the disturbance, and these are omitted for the sake of brevity. However, the resulting data have been used to construct neutral curves based on the various measures. Figures 4a and 4b show such curves for $\tau_0 = 1$ and $\tau_0 = 10$, respectively.

In Fig. 4a, it is clear that the different measures yield different stability criteria. In all but one of the four measures, the region of instability is larger than that given by the approximate theory. As mentioned earlier, the approximate theory relies on the whole thermal profile reaching a minimum amplitude simultaneously, a strong restriction. The heat transfer measures are local measures and may not necessarily account fully for the global evolution of the disturbance with time, such as different internal variations of the temperature profile. The thermal energy measure is a global measure, and this yields the largest region of instability. Careful computations using much smaller steps in τ and finely graded values of k yield the following minimum values:

$$\tau_c = 8.9018, \quad k_c = 0.07807 \tag{18}$$

These values should be compared with those given in (15), which correspond to quasi-steady approximate theory. Although there is some difference in the

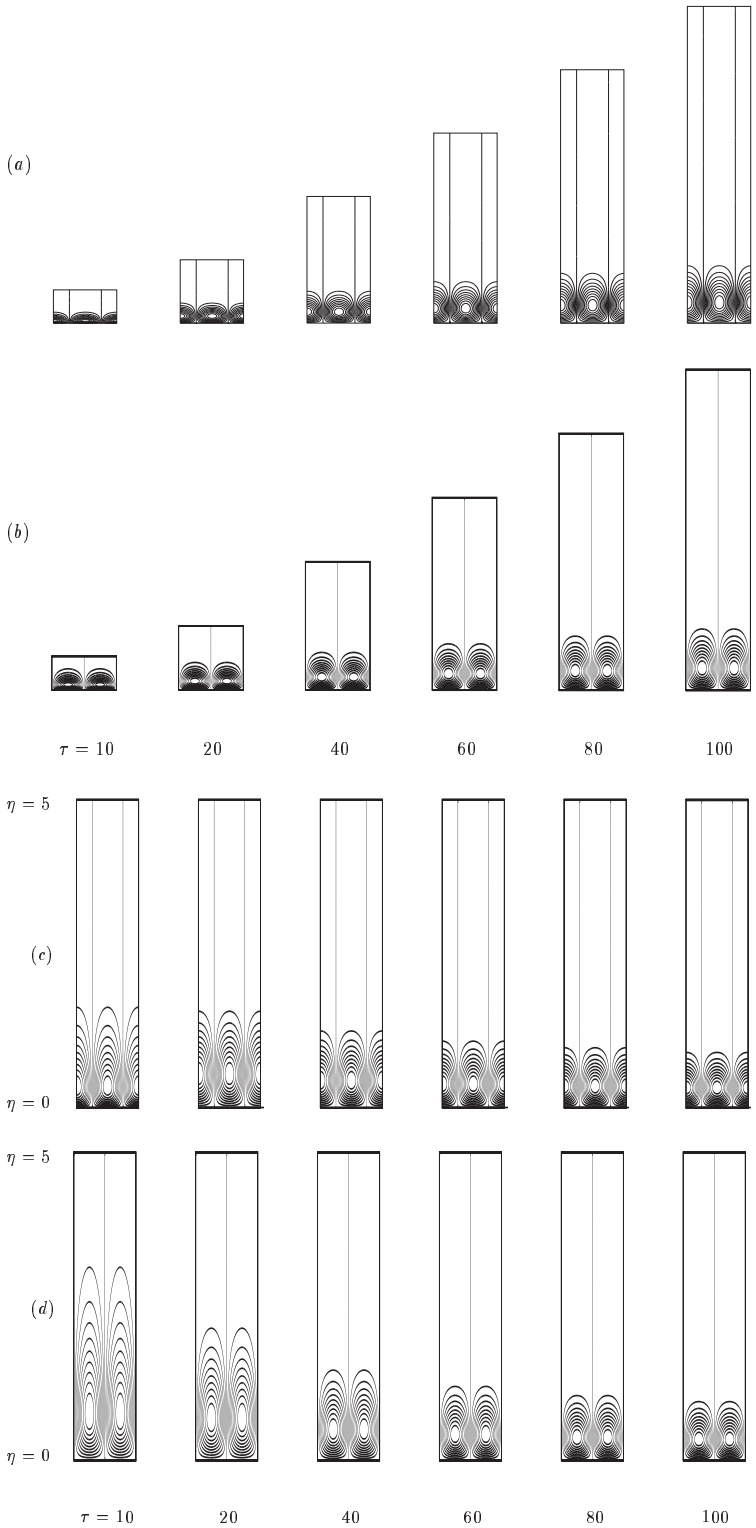

Figure 2. Disturbance isotherms and streamlines corresponding to the wave number $k = 0.06$ for various values of τ with $\tau_0 = 10$: **a)** isotherms in (x, y); **b)** streamlines in (x, y); **c)** isotherms in (x, η); and **d)** streamlines in (x, η)

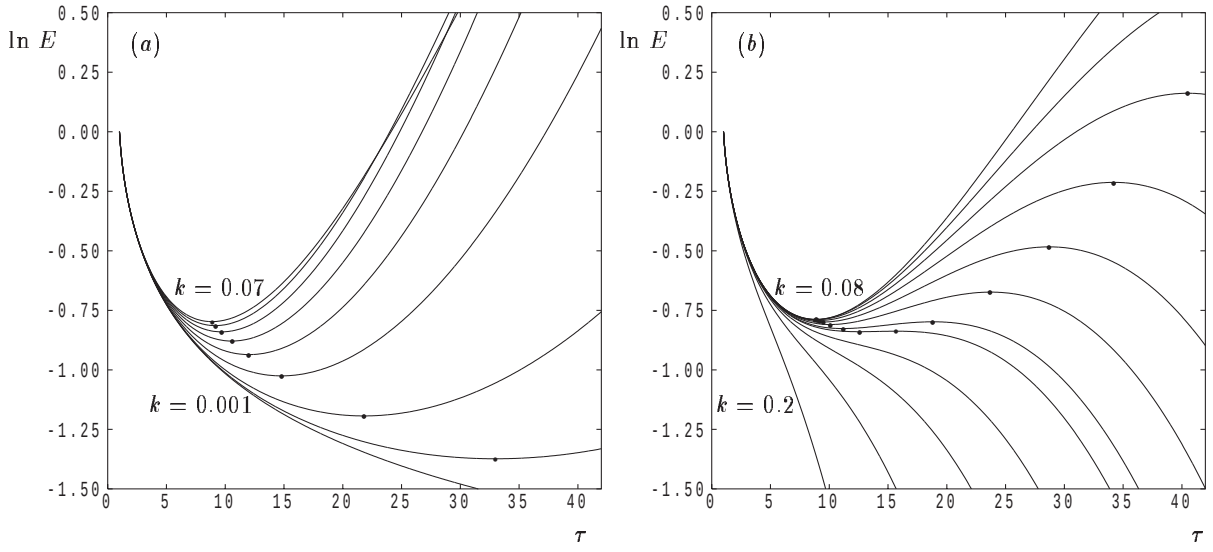

Figure 3. Variation of $\ln E$ against τ for different values of k. The symbol $\bullet$ denotes maximum and minimum values of E: **a)** $k = 0.001,\ 0.005,\ 0.01,\ 0.02$,...,$0.07$; **b)** $k = 0.09,\ 0.10,\ 0.11$,...,0.20

critical wave numbers, the neutral curves are fairly flat near their minima, and therefore, the discrepancy between the critical wave numbers is unlikely to be of great significance. On the other hand, given that $t = \tau^2$, the critical times obtained from (15) and (18) are 167.56 and 78.24, respectively. Therefore, there is a very large discrepancy between the approximate and the exact theories in this regard.

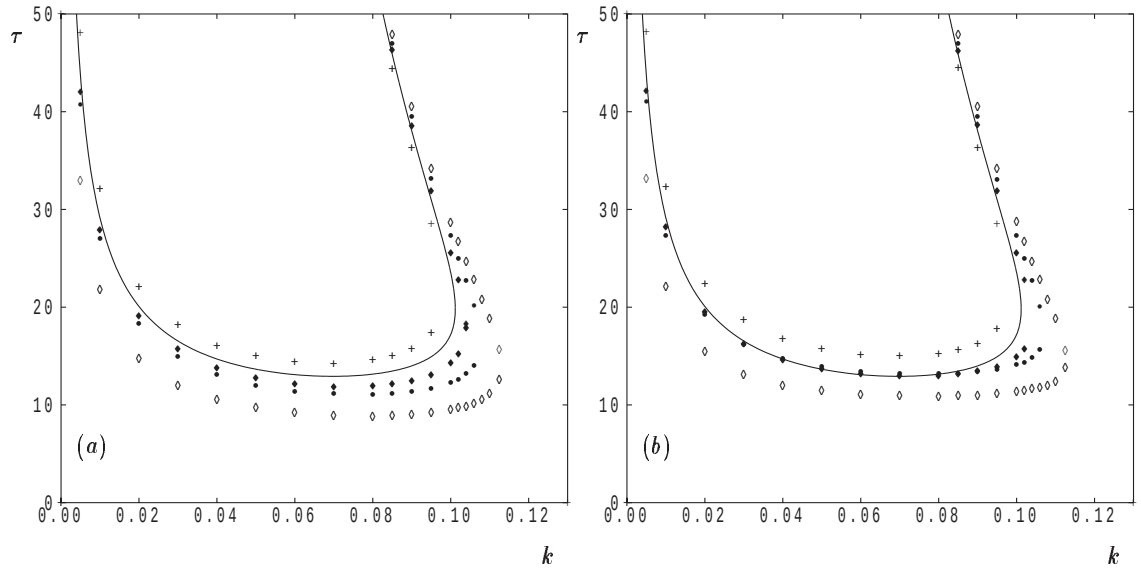

Figure 4. Neutral stability giving τ_c as a function of k. The continuous curve represents the approximate theory as displayed in Fig. 1b. The symbol $\diamond$ represents the thermal energy stability criterion. The symbols $\bullet$ and $+$ represent the surface heat flux criterion in terms of η and y, respectively. The symbol $\blacklozenge$ represents the maximum temperature criterion. The disturbance is introduced at **a)** $\tau_0 = 1$ and **b)** $\tau_0 = 10$

Figure 4b shows the modifications to the neutral points brought about by changing τ_0 from 1 to 10. Once more, the energy measure yields the largest region of instability, but the primary effect of a later initiation time is that the instability is suppressed and occurs later. This observation quite naturally leads to the question of the role played by the initiation time, and since the disturbance profile varies with τ, by the initial profile shape.

Figure 5a shows the evolution of the disturbance energy corresponding to the initiation times, $\tau_0 = 1, 2, ..., 15$ for the fixed wave number $k = 0.085$. The values of τ_c are also depicted using filled circles. This figure shows that each curve has its maximum value at the same value of τ whenever the disturbance is introduced within the chosen range of initiation times, but that the minima, which correspond to the onset of convection, vary with τ_0. A closer look at Fig. 5a suggests that the onset time hardly varies with τ_0 when $\tau_0 \leq 5$, which suggests that the disturbance now has sufficient time to evolve into a common solution trajectory by the onset time when τ_0 is sufficiently small.

An alternative view of Fig. 5a is given in Fig. 5b, where the energies are normalized to have the same values at $\tau = 20$; this is a valid process since linearized theory takes no account of absolute magnitudes. This figure shows more clearly the effect of the different initiation times, and the common trajectory, which is taken once transients caused by the arbitrary choice of initial condition have died out. Although we do not show it, it is clear that an initiation time that is later than the time corresponding to the maxima in Figs. 5a and 5b results in a disturbance that decays.

Turning our attention to different disturbance shapes, we now consider thermal disturbances in the form $\eta e^{-(\eta-\eta_0)^2}$ where η_0 denotes the midpoint of the disturbance. Therefore, we are able to define disturbances that are centered in the region outside the basic thermal boundary layer. These disturbances are initiated at $\tau_0 = 1$ for $k = 0.1$. Figure 6 shows how the evolving temperature profile varies with τ when $\eta_0 = 6$. This case, which is typical, shows that disturbances that are detached from the heated surface migrate quickly toward the surface. For the particular case chosen, this process takes place in the very short time interval $1 < \tau < 3$. A similar behaviour ensues for other choices of η_0.

Although the distubance migrates quickly toward the hot surface, the shape of the disturbance takes

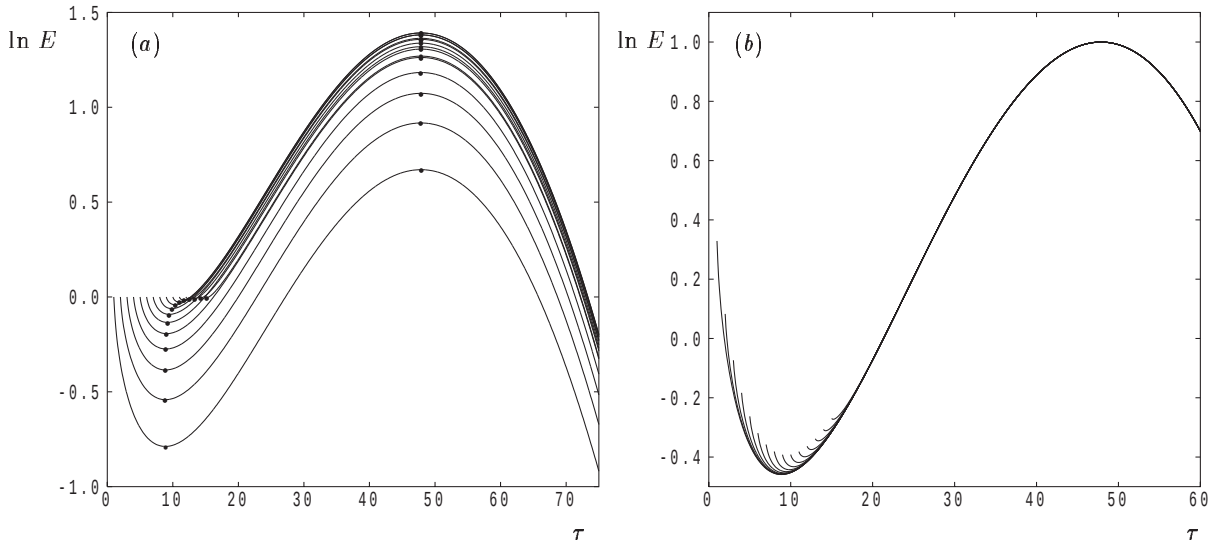

Figure 5. Variation of $\ln E$ against τ for disturbances introduced at various values of τ_0. The disturbance wave number is $k = 0.085$: **a)** Computed $\ln E$ curves; **b)** normalized $\ln E$ curves

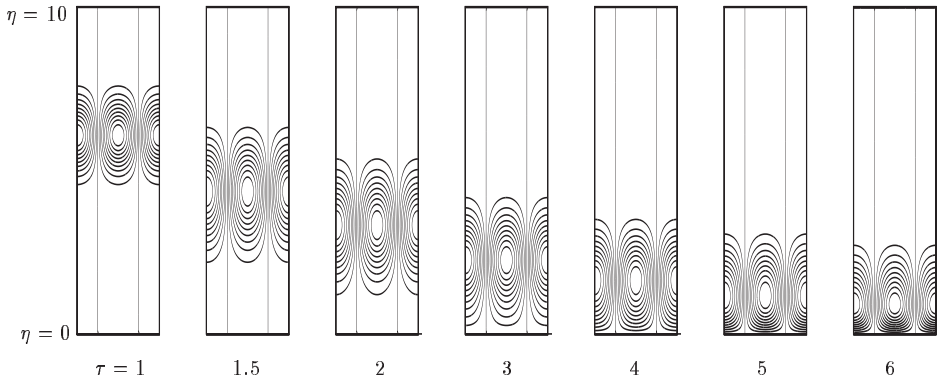

Figure 6. Contours in (x, η)-space of the thermal disturbance profile at different times. The initial disturbance takes the form $\eta e^{-(\eta-6)^2}$, is introduced at $\tau_0 = 1$, and has wave number $k = 0.1$

longer to attain than that of the common trajectory. The approach to the common trajectory for different values of η_0 is shown in Fig. 7 for $\eta_0 = 0, 2, 4,$ and 6. Figure 7a shows the computed thermal energies while Fig. 7b shows the normalized energies. The decay of transients is essentially complete, and the energy curves are virtually identical just before the neutral time at $\tau \simeq 10$. It is important to note that there are spurious maxima at small values of τ shown in Fig. 7 for the cases $\eta_0 = 4, 6$. These maxima should not be interpreted as marking the transition from instability to stability. Rather, given the form of thermal profiles shown in Fig. 6, we see that the disturbance elongates in the η direction as it moves toward the heated surface, and this causes the apparent rise in the energy. In this context, it is important to note that the corresponding surface heat transfer curves would show a much larger initial increase as τ increases from τ_0 because the initial large-η_0 disturbances have negligible surface heat transfer until the disturbance approaches the surface. Therefore, the spurious instability will appear to be much stronger when considering the surface rate of heat transfer as the basis of a stability criterion.

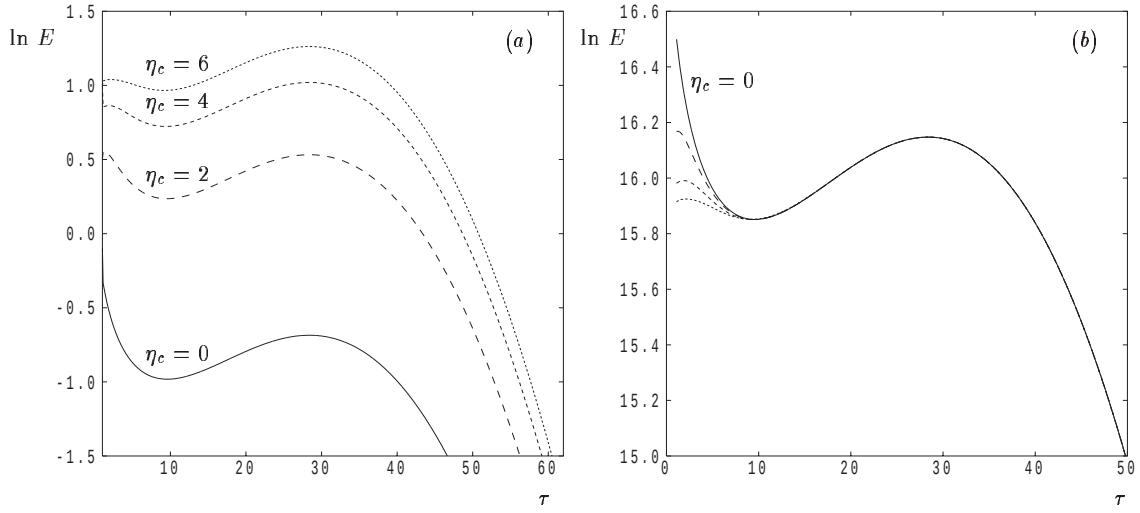

Figure 7. Variation of $\ln E$ against τ for initial disturbances of the form $\eta e^{-(\eta-\eta_0)^2}$ for $\eta_0 = 0$, 2, 4 and 6: **a)** Computed $\ln E$ curves; **b)** normalized $\ln E$ curves

DISCUSSION AND CONCLUSIONS

In this paper, we have sought to understand the stability characteristics of the conductive thermal boundary layer, which arises above a suddenly heated horizontal surface in a porous medium. To this end, we have developed both an approximate theory and an exact theory. In the latter case, various measures of the amplitude of the evolving disturbance have been proposed and used.

We have found that the approximate theory gives a typically shaped neutral curve for which there is a maximum wave number above which all disturbances decay with time. The minimum time before which disturbances may grow, under the constraints of the approximate theory, is given in Eq. (15). However, we cannot compare this result to that of Kim et al. (2003) who undertook the study of what is essentially the same mathematical problem, although the application cited was one of mass diffusion, rather than thermal diffusion. The minimum critical time computed by Kim et al. (2003) and its associated wave number are given by

$$\tau_c = 7.2662, \qquad k_c = 0.07426 \tag{19}$$

where we have presented the data in our notation and have recomputed their values in order to have more significant figures. These values are quite different from those given in (15), but the reason for this is that Kim *et al.* (2003) used slightly different boundary conditions. Although the temperature perturbation is zero on $y = 0$, they invoke a 'stress-free' boundary condition, $\partial v/\partial y = 0$, which may be translated into $\partial\psi/\partial y = 0$ in the present context. Thus their configuration corresponds to a horizontal surface through which the fluid disturbance may pass vertically, but which has a zero disturbance temperature. It is difficult to see how this condition might be set up in practice, but it does mean that their work and ours cannot be compared directly.

In general, for the full parabolic simulations, we have found that the initial shape and the initiation time have no effect on the transition from stability to instability, i.e. on the critical time, but only if the initiation time is sufficiently early that the disturbance has evolved to a common evolutionary trajectory. We have also found that there is some degree of arbitrariness in defining what is meant by instability in an evolving context for different measures of the amplitude of the disturbance give different neutral curves. Indeed, we have shown that the thermal energy measure yields a critical time which is much earlier than those obtained using either quasi-static theory or other measures of the strength of the evolving disturbance. In addition, and perhaps more importantly, the energy criterion is a global criterion and we would regard it as being more well-suited as a measure of the overall evolution of the disturbance. Therefore we would suggest that the energy criterion should be used as the measure of the amplitude of the evolving disturbance in unsteady basic flows.

It is now possible to extend the present work to the following situations: (i) Darcy-Brinkman convection, (ii) cases where local thermal nonequilibrium applies and (iii) double diffusive cases. The third situation will be of the most interest, for in the Darcy-Bénard context there are parameter regimes whether the most unstable mode undergoes a Hopf bifurcation at onset. Thus there is the possibility of novel qualitative effects.

However, our present aim is to extend the above work into the nonlinear regime. The authors have developed a nonlinear two-dimensional code to study the evolution of large amplitude disturbances. That analysis may be found in Selim & Rees (2007), but work on three-dimensional instabilities is ongoing.

ACKNOWLEDGMENT

The first author would like to thank the University of Bath for a Departmental Studentship and an Overseas Research Award to enable this research to be undertaken.

REFERENCES

Bassom, A. P., and Blennerhassett, P. J., Impulsively generated convection in a semi-infinite layer above heated flat plate, *Q. J. Mech. Appl. Math.*, vol. **55**, no. 4, pp. 573–595, 2002.

Cheng, P., and Chang, I. D., Buoyancy induced flow in a porous medium adjacent to impermeable horizontal boundaries, *Int. J. Heat Mass Transfer*, vol. **19**, pp. 1267–1272, 1976.

Cheng, P., and Minkowycz, W. J., Free convection about a vertical flat plate embedded in a porous medium with application to heat transfer from a dike, *J. Geophys. Res.*, vol. **82**, pp. 2040–2044, 1977.

Choi, C. K., Kang, K. H., Kim, M. C., and Hwang, I. G., Convective instabilities and transport properties in horizontal fluid layers, *Korean J. Chem. Eng.*, vol. **15**, pp. 192–198, 1998.

Foster, T. D., Stability of homogeneous fluid cooled uniformly from above, *Phys. Fluids*, vol. **8**, pp. 1249–1257, 1965.

Horton, C. W., and Rogers, F. T., Convection current in a porous media, *J. Appl. Phys.*, vol. **16**, pp. 367–370, 1945.

Hwang, I. G., and Choi, C. K., An analysis of the onset of compositional convection in a binary mixture solidified from below, *J. Cryst. Growth*, vol. **162**, pp. 182–189, 1996.

Kaviany, M., Thermal convective instabilities in a porous medium, *ASME J. Heat Transfer*, vol. **106**, pp. 137–142, 1984.

Keller, H. B., and Cebeci, T., Accurate numerical methods for boundary layer flows 1. Two dimensional flows, *Proc. Int. Conf. Numerical Methods in Fluid Dynamics*, Lecture Notes in Physics, Springer, New York, 1971.

Kim, M. C., Choi, K. H., and Choi, C. K., Onset of thermal convection in an initially stably stratified fluid layer, *Int. J. Heat Mass Transfer*, vol. **42**, pp. 4253–4258, 1999.

Kim, M. C., and Kim, S., Onset of convective instability in a fluid-saturated porous layer subjected t o time-dependent heating, *Int. J. Heat Mass Transfer*, vol. **32**, pp. 416–424, 2005.

Kim, M. C., Kim, S., and Choi, C. K., Convective instability in fluid-saturated porous layer under uniform volumetric heat sources, *Int. Comm. Heat Mass Transfer*, vol. **29**, no. 7, pp. 919–928, 2002.

Kim, M. C., Kim, S., Chung, B. J., and Choi, C. K., Convective instability in a horizontal porous layer saturated with oil and a layer of gas underlying it, *Int. Comm. Heat Mass Transfer*, vol. **30**, no. 2, pp. 225–234, 2003

Kim, M. C., Chung, T. J., and Choi, C. K., The onset of Taylor-like vortices in the flow induced by an impulsively started rotating cyclinder, *Theor. Comput. Fluid Dyn.*, vol. **18**, pp. 105–114, 2004.

Lapwood, E. R., Criterion for the onset of convection flow in a fluid in a porous media, *Proc. Camb. Phil. Soc.*, vol. **44**, pp. 508–521, 1948.

Lewis, S., Bassom, A. P., and Rees, D. A. S., The stability of vertical thermal boundary layer flow in a porous medium, *Eur. J. Mech. B*, vol. **14**, pp. 395–408, 1995.

Lewis, S., Rees, D. A. S., and Bassom, A . P., High wave number convection in tall porous containers heated from below, *Q. J. Mech. Appl. Math.*, vol. **50**, pp. 545–563, 1997.

Morton, B. R., On the equilibrium of a stratified layer of fluid, *J. Appl. Math.*, vol. **10**, pp. 433–447, 1957.

Rees, D. A. S., Nonlinear wave stability of vertical thermal boundary layer flow in a porous medium, *Z. Appl. Math. Phys.*, vol. **44**, pp. 306–313, 1993.

Rees, D. A. S., Thermal boundary layer instabilities in porous media: A critical review, *Transport Phenomena in Porous Media*, Ingham, D. B. & Pop, I., (eds.), Pergamon, London, pp. 233–259, 1998.

Rees, D. A. S., The stability of Darcy–Bénard convection, *Handbook of Porous Media*, K. Vafai, ed., Marcel Dekker, New York, pp. 521–558, 2000.

Rees, D. A. S., *Stability Analysis of Darcy-Bénard Convection*, Lecture Notes from the Summer School on Porous Medium Flows, Neptun, Constanţa, Romania, June, 25–29, 2001a.

Rees, D. A. S., Vortex instability from a near-vertical heated surface in a porous medium. I Linear theory, *Proc. Roy. Soc. A.*, vol. **457**, pp. 1721–1734, 2001b.

Rees, D. A. S., *Recent advances in porous medium thermal boundary layer instabilities*, Transport Phenomena in Porous Media II, Ingham, D. B. and Pop, I., (eds.), Pergamon, London, pp. 54–81, 2002a.

Rees, D. A. S., Vortex instability from a near-vertical heated surface in a porous medium. II Nonlinear theory, *Proc. Roy. Soc. A.*, vol. **458**, pp. 1575–1592, 2002b.

Rees, D. A. S., Nonlinear vortex development in free convective boundary layers in porous media, *NATO ASI Proceedings*, Neptun, Romania, June 9–20, pp. 449–458, 2003.

Rees, D. A. S., and Bassom, A. P., The nonlinear nonparallel wave instability of free convection induced by a horizontal heated surface in fluid-saturated porous media, *J. Fluid Mech.*, vol. **253**, pp. 267–296, 1993.

Selim, A., and Rees, D. A. S., The stability of a developing thermal front in a porous medium. II Nonlinear Evolution, J. Porous Media, vol. **10**, no. 1, pp. 2–10, 2007.

Storesletten, L., and Rees, D. A. S., The influence of higher-order effects on the linear instability of thermal boundary layer flow in porous media, *Int. J. Heat Mass Transfer*, vol. **41**, pp. 1833–1843, 1998.